university of groningen / faculty of science and engineering

SSZ-13 catalyst for the Methanol-to-Olefins process: effect of reaction temperature, weight hourly space velocity and methanol partial pressure

Sara Maljkovic
S4043383
Supervisor: Dr. ir. Jingxiu Xie

June 23, 2022

Chemical Engineering
Bachelor Research Project (WBCE901-15)

Abstract

The Methanol-to-Olefins process allows for an alternative way of lower olefin (C_2 to C_4) production over a zeolite catalyst. The aim of this research was to study the influence of the reaction conditions (reaction temperature, weight hourly space velocity and methanol partial pressure) on the catalytic performance and products of the process, using a fixed-bed reactor. The SSZ-13 zeolite was employed as the catalyst. It was analysed by X-Ray Diffraction (XRD) and Ammonia-Programmed Temperature Desorption (NH_3-TPD) to confirm its chabazite topology and its acidity. The varying of reaction conditions gave rise to different methanol conversions and product compositions. When decreasing the WHSV from 1.03 h^{-1} to 0.77 h^{-1}, the catalytic lifetime increased from 3 to 4 hours. When increasing the methanol partial pressure by 0.1 bar, the lifetime of the catalyst doubled from 2.5 hour to 5 hours. Catalytic lifetime was longest for intermediate temperatures (390°C and 430°C), as at high and low temperatures, catalyst deactivation was the quickest. Aside from the lower olefins, pentene and paraffins (C_1 to C_4) were also produced. The selectivity towards ethylene and propylene increased throughout the reaction, while the selectivity towards butene and pentene decreased thought out the reaction. The spent catalyst samples were analysed with XRD. The spent catalyst framework shifted and its crystalinity decreased. The amount of hydrocarbon material retained within the catalyst after the reaction was established with Thermogravimetric Analysis (TGA). Reaction conditions were found to have an important influence on catalyst deactivation rate, retention of hydrocarbon material and product compositions.

1 Introduction

Hydrocarbons were for years, and still are now, obtained from crude oil, and used mostly as fuel. However, in the late 1970s, the energy and oil crisis incited research on alternative ways to produce hydrocarbons. This is when the Methanol-to-Hydrocarbon (MTH) process emerged [1]. This process involves the reaction of methanol, over a zeolite catalyst to obtain hydrocarbons. With catalyst type and reaction conditions, the MTH process was tuned to give rise to the Methanol-to-Gasoline (MTG) process and the Methanol-to-Olefins (MTO) process [2]. The latter was investigated during this research. The desired products of the MTO process are lower olefins (C_2 to C_4), which are the building blocks of the petrochemical industry. Methanol can today be made from sustainable carbon feed stocks such as industrial CO_2 and municipal waste, allowing for the MTO process to contribute to a circular carbon economy.

The zeolite ZSM-5 was first employed as catalyst for the MTH process. However, it was later discovered that by using SAPO-34, lower olefins would be the

main product of the reaction [2]. Another competitor of SAPO-34 that became interesting for the production of light olefins was SSZ-13. These two catalysts are isostructural with a chabazite (CHA) topology. However, SAPO-34 is a silicoaluminophosphate zeolite (containing Al, Si, P, and O atoms) while SSZ-13 is a aluminosilicate zeolite (containing only Al, Si and O atoms). SSZ-13 also has a lower aluminum content than SAPO-34, with an Si/Al ratio between 20 and 30 [3]. This leads to a stronger acidity for SSZ-13, and in turn a higher catalytic activity than SAPO-34 [4]. Therefore, during this research, the commercial SSZ-13 zeolite was used. The activity of a zeolite catalyst is due to both Brønsted and Lewis acid sites within the catalytic pores. The conversion of methanol however happens within the stronger acid sites [2].

Zeolite catalysts are defined as microporous, aluminosilicate materials that are used to increase the rate of chemical reactions. The building blocks of SSZ-13 are SiO_4 and AlO_4 tetrahedra, each connected with an oxygen atom [5]. This allows for a three-dimensional framework. This framework plays an important role in the MTO process, as it in part dictates the selectivity towards different types of olefins. The specific CHA topology, mentioned earlier, consists of alternating SiO_4 and AlO_4 tetrahedrons that form eight-membered rings [3]. As can be seen from Figure 1, these eight-membered rings are connected and constitute the windows to the zeolite pores.

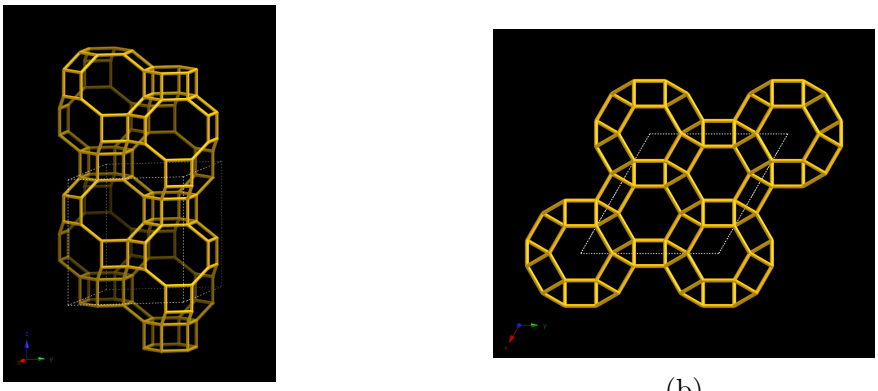

(a) (b)

Figure 1: CHA framework viewed (a) normal to [001] and (b) along [001] [6].

The size of these windows explains why catalysts with CHA topology are widely used for the MTO process. The windows are the entry point to the internal channel system of the zeolite. For the CHA type framework, the diameter of the windows and pores is quite small (3.72 Å [6]). Smaller molecules, such as ethylene and propylene, will be able to pass through the catalytic channels. Larger molecules, higher olefins and aromatics, on the other hand will get trapped within the pores and cavities [2]. SSZ-13 is therefore shape selective towards lower olefins, which is why it is used for the MTO process.

The mechanism for the formation of alkenes in the MTO process is continuously undergoing research. However, the two main steps are as follows; methanol is first partially dehydrated to dimethyl ether (DME), followed by the formation of alkenes in a so called "hydrocarbon pool" [2][7]. The hydrocarbon pool refers to the variety of different hydrocarbons, including aromatics, higher alkenes and parrafins, formed within the catalyst. This hydrocarbon pool, first proposed by Dahl and Kolboe [8], became of great importance as the auto-catalytic properties of the MTO reaction were discovered. By auto-catalytic, it is meant that the reaction between the C_1 compounds (methanol and DME) and the hydrocarbon pool is more favorable than the formation of a new C-C bond from two C_1 compounds. The simultaneous dual-cycle concept, shown in Figure 2, was then introduced. According to these two mechanistic cycles, light olefins are formed from either the olefin-based cycle, where methylation and cracking of higher olefins happens or from the aromatic-based cycle where lower olefins can split off from methylbenzenes (dealkylation) [2][7][9].

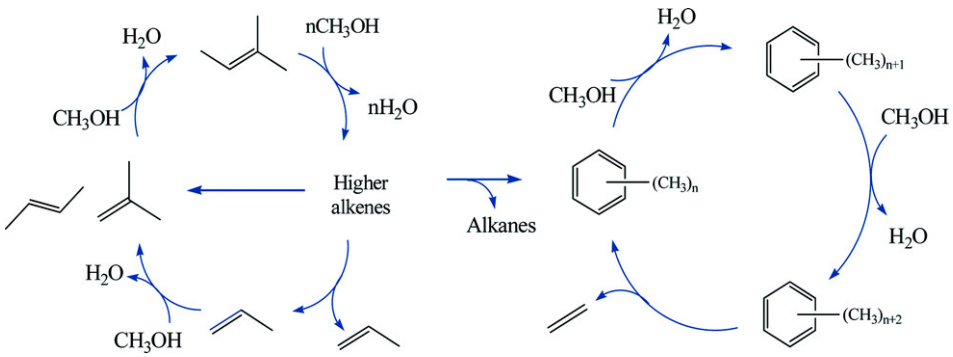

Figure 2: Dual-cycle mechanism proposed by Dahl and Kolboe [2].

The dual-cycle mechanism also shows that the main side products of the MTO reaction are alkanes, with propane being the largest contributor [2].

A major problem encountered during the MTO process is catalytic deactivation due to coke formation, inhibiting the production of olefins. As the reaction, proceeds, the larger molecules formed within the hydrocarbon pool (aromatics, polyaromatics) become trapped within the small catalytic pores and block the acid sites. Gradually, the hydrocarbons are converted into graphitic type coke. This decreases catalytic activity and leads to deactivation [7].

As mentioned earlier, the selectivity towards lower olefins is in part due to the the zeolite structure, however the reaction conditions also have an important influence. By changing the reaction conditions, the methanol conversion and selectivity towards specific alkenes can be tuned. The goal of this research was to modify the temperature, weight hourly space velocity and methanol partial pressure and investigate their influence on the catalytic performance, including activity, selectivity and stability.

2 Experimental

2.1 Catalyst preparation and characterization

The commercial zeolite SSZ-13, supplied from ACS materials, was first calcined at 550°C for 5 hours to obtain the catalyst in its H form. The calcined catalyst was then pressed under a 2 metric ton load to obtain pellets. These pellets were crushed using a mortar and pestle and sieved to a sieve fraction of $212 - 425$ μm. This fraction was transferred to a closed vial and was used for testing the reaction conditions.

The catalyst in its H form was characterized by its crystallinity and acidity. X-Ray powder diffraction (XRD) was used to determine the crystallinity and framework of the catalyst. The XRD pattern of the sample was recorded between 5 °and 50°(2θ angles) at room temperature [10], on a Bruker D-8 Advance-Germany Spectrometer, using Cu-Kα radiation ($\lambda = 1.5418$ Å) generated at 40 kV and 40 mA. The obtained diffraction pattern was then compared to the standard diffraction pattern for CHA-type zeolites. Moreover, to determine the influence of coke formation on the framework, the spent catalyst sample after experiment 8 (see Table 1) was analysed with XRD under the same conditions. The patterns for the fresh catalyst and the spent catalyst were compared.

Ammonia temperature-programmed desorption (NH_3-TPD) was used to determine the number of weak and strong acid sites within the catalyst. A Micromeritics AutoChem II 2920 apparatus equipped with a thermal conductivity detector (TCD) was used for performing the NH3–TPD measurement. Firstly, 0.1 g of the sample was treated at 550° C under the Helium atmosphere. Next, ammonia desorption was carried out (with 10 % vol. NH3 in He stream) from 100 to 600 °C. The TCD signal obtained was plotted against the temperature. The result was compared to literature to see whether the catalyst exhibited the desired acidity.

2.2 Reaction condition testing

To test the reaction conditions on the MTO process, the reaction set-up shown in the P&ID in Figure 3 was used. The main piece equipment is the fixed-bed reactor which is surrounded by a cylindrical oven. For this research, a glass reactor was used, however according to Borodina et al.[10] and Dai et al.[11], a quartz or stainless steel reactor are usually preferred. The liquid methanol is contained in a saturator, heated with a water bath and is carried to the inlet of reactor using a nitrogen (N_2) flow. The lines to and from the reactor are at 80°C to ensure full vaporization of methanol. The products from the reaction are passed through a cooler and sent to an online gas chromatography (GC) column. In the set up, multiple by-passes and check valves are present to ensure the safe and desirable operation of the process. For more details, see the HAZOP study in Appendix A.

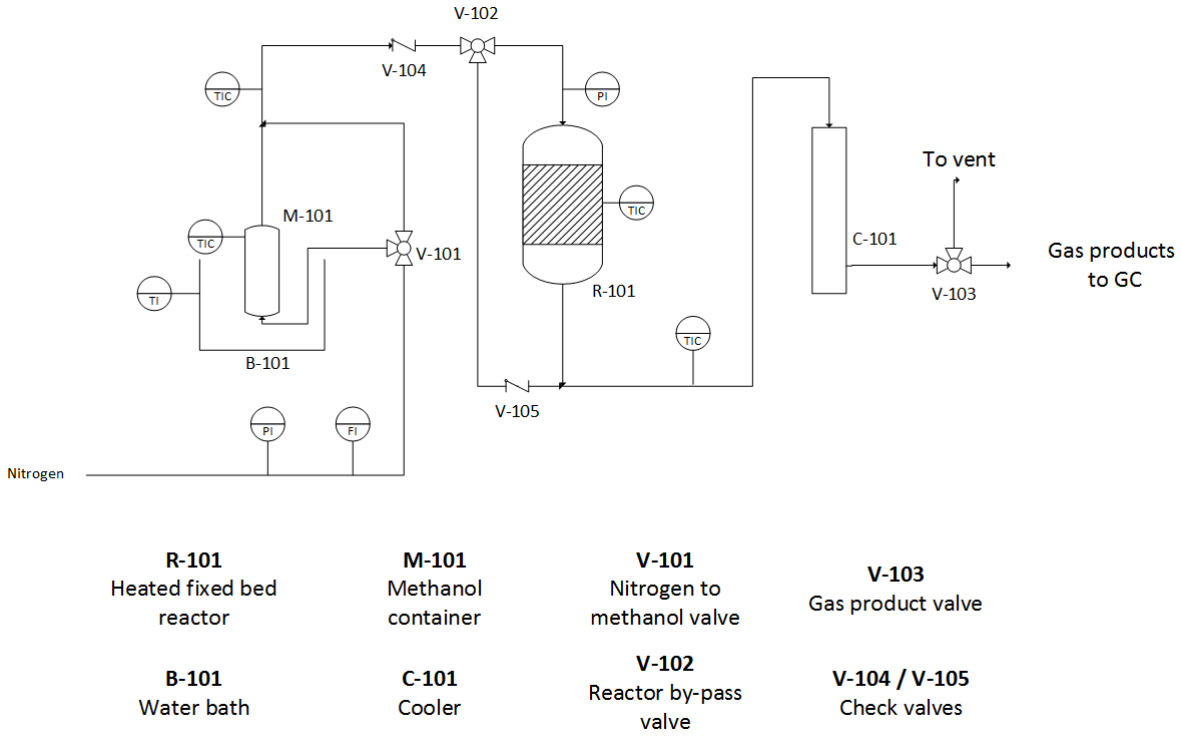

Figure 3: P&ID of reaction set up

A total of nine experiments were conducted for this research. The three reaction parameters that were changed are: the reaction temperature, the weight hourly space velocity (WHSV) and the methanol partial pressure. To calculate the necessary methanol partial pressure, methanol flow rate and WHSV, the equations presented below were used.

To find the volumetric flow rate of methanol, the partial pressure of methanol was first found with the Antoine Equation (1).

$$\text{Antoine Equation:} \qquad log_{10}P_{MeOH} = A - \frac{B}{C+T} \tag{1}$$

with A = 5.20409, B = 1581.341, C = -33.5 and the temperature T of methanol saturator in Kelvin.

$$\text{Total pressure:} \qquad P_{total} = P_{MeOH} + P_{N_2} \tag{2}$$

with P_{total} = 1 bar.

$$\text{Total flow rate:} \qquad \Phi v_{total} = \Phi v_{MeOH} + \Phi v_{N_2} \tag{3}$$

$$\text{Methanol flow rate:} \qquad \Phi v_{MeOH} = \Phi v_{total} * P_{MeOH} \tag{4}$$

The ideal gas law was used to find the total molar flow rate of methanol to the reactor.

$$\text{Ideal gas law:} \qquad P_{total} * \Phi v_{total} = \Phi mol_{total} * R * T \tag{5}$$

$$\text{Methanol molar flow rate:} \qquad \Phi mol_{MeOH} = \Phi mol_{total} * P_{MeOH} \tag{6}$$

$$\text{Methanol mass flow rate:} \qquad \Phi m_{MeOH} = \Phi mol_{MeOH} * M(MeOH) \tag{7}$$

with M(MeOH) = 32.04 g/mol.

$$\text{WHSV} = \frac{\Phi m_{MeOH}}{catalyst\ mass} \tag{8}$$

The units of the methanol mas flow rate are in g/h and the catalyst mass in grams, leading to a WHSV with units of h^{-1}.

A summary of all experiment can be seen in Table 1. Note that the experiment at 470°C was repeated three times to check for reproducibility.

Experiment	Temperature (^{o}C)	Catalyst loading (mg)	WHSV (h-1)	MeOH partial pressure (bar)
1	430	300	1.03	0.165
2	390	300	1.03	0.165
3	470	300	1.03	0.165
4	430	200	1.54	0.165
5	430	400	0.77	0.165
6	350	300	1.03	0.165
7	430	530	1.03	0.266
8	470	300	1.03	0.165
9	470	300	1.03	0.165

Table 1: Summary of all experiments

First, the thermocouple in the reactor was removed and the reactor was taken out of the oven. The reactor was filled with a little bit of quartz wool, followed by the desired amount of catalyst (see table 1). The reactor was placed back inside the oven and the cleaned thermocouple was inserted inside. The water bath was heated to the desired temperature (24.5°C for 0.165 bar and 34.5°C for 0.266 bar). The valves were turned to allow only N_2 flow through the reactor. The N_2 flow was set to 20 ml/min. To check for any leaks, the valve leading to the GC was closed and the system was pressurized to 60-80 mbar by turning the N_2 flow off. If after 5 minutes there was no pressure drop, the valves were opened and the system was allowed to stabilize. The oven temperature was then set to the desired temperature (set point was 80°C higher than actual temperature in reactor) and left to heat up for an hour. While heating of the reactor, the GC sequence for the experiment was built. Once the reactor had reached the desired temperature, the N_2 flow was allowed through the methanol saturator and after five minutes, the online GC was started. For each experiment, a sample was injected every 40 minutes. If after 6 hours on stream, the GC still showed lower olefins in the product stream, the reaction was left over night. The spent catalyst

was collected the next day in a vial to keep for analysis. For each experiment the same procedure was repeated, only varying the parameter that needed to be changed. The temperature was varied by changing the oven temperature, the WHSV was varied by changing the catalyst loading and the methanol partial pressure was varied by changing the temperature of the methanol saturator.

2.3 Product Analysis

As mentioned above, the gaseous products were analysed using an online GC. For each injection, the relative area of each component detected by the flame ionizing detector (FID) was looked at. To distinguish the propylene and propane areas, the ratio of the two detected by the thermal conductivity detector (TCD) was used. These areas were then plotted per experiment to give rise to the graphs shown in *"3 Results and Discussion"*. All the calculations regarding methanol conversion and product selectivities are show below.

$$\text{MeOH Conversion: } \frac{100 - Relative\ Area_{MeOH} - Relative\ Area_{DME}}{100} \tag{9}$$

$$\text{Olefin Selectivty: } \frac{Relative\ Area_{olefin}}{MeOH\ Conversion} \tag{10}$$

$$\text{Alkane Selectivity: } \frac{Relative\ Area_{alkane}}{MeOH\ Conversion} \tag{11}$$

$$\text{Butene Isomer Selectivity: } \frac{Butene\ isomer\ relative\ area}{Total\ butane\ area} \tag{12}$$

To determine the coke content on the spent catalysts, thermogravimetric analysis (TGA) was performed. For TGA, the spent catalyst sample was first heated up from room temperature to 600°C (ramp of 10°C/min). It was then held at 600°C for an hour, under air flow. TGA was done for the spent catalyst of Experiments 1 through 7.

3 Results and Discussion

3.1 Catalyst Characterization

3.1.1 X-Ray Powder Diffraction

An XRD analysis of the commercial fresh catalyst was performed to confirm its structure and crystallinity with that of the CHA-type framework zeolite. According to ACS Materials LLC [3], the relative crystallinity of the zeolite is above 90%, with its characteristic peaks being at 9.38°, 12.78°, 20.42°, 22.86°, 24.56°, 30.34° and 30.74° (2θ angles) [6]. The XRD patterns of a reference CHA zeolite and the H-SSZ-13 sample used for the research are compared in Figure S1 in Appendix B. When the two are overlapped, it can be seen that the amount and

general position of the peaks are the same for both patterns. However, all of the H-SSZ-13 sample peaks are shifted to the right. This peak shift could indicate that the unit cell dimensions of the tested sample are slightly different than for the ideal CHA zeolite [12]. However, as it is a systematic shift, it can still be confirmed that the tested H-SSZ-13 sample posses a CHA topology.

To see how the framework and crystallinity are affected by the MTO reaction, the XRD patterns of the fresh and spent catalyst after experiment 8 (see Table 1) are compared in Figure 4.

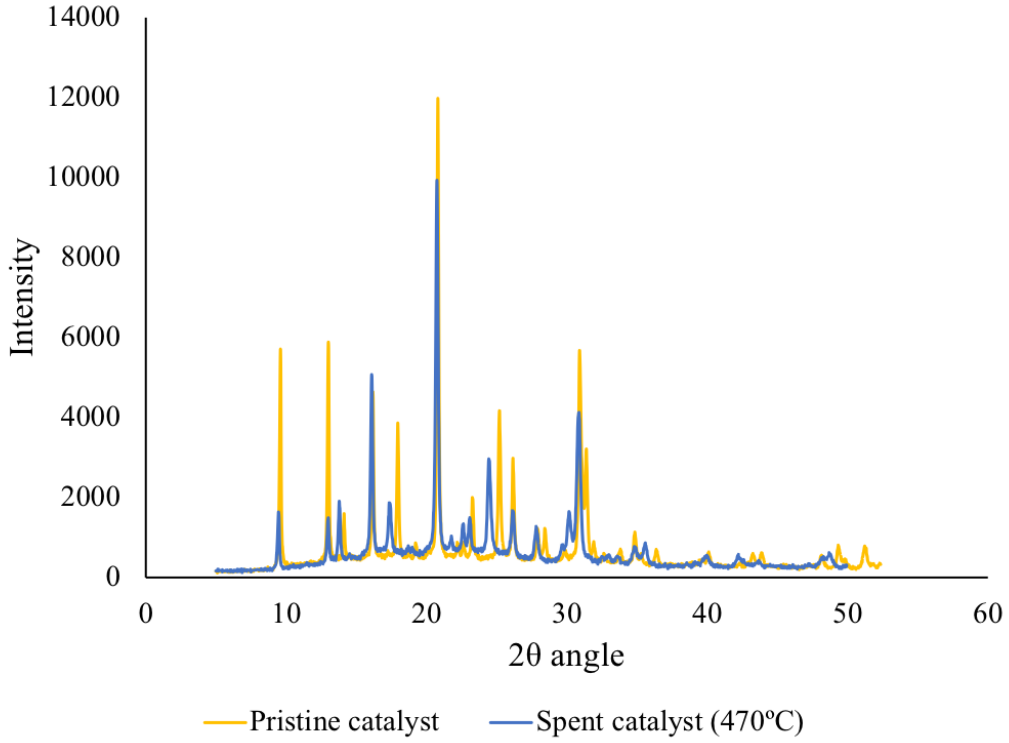

Figure 4: XRD patterns of the fresh catalyst and spent catalyst at 470°C.

Some of the peaks from the spent catalyst overlap with the peaks from the fresh catalyst, however at the 2θ angles of 18°, 25°and 29°, the spent catalyst peaks are shifted to the left. This indicates that the framework of the H-SSZ-13 catalyst is affected by the MTO reaction. This is due to the formation of aromatic molecules that are trapped within the catalytic pores. As explained by J.Goetze et al.[13], the size of the retained hydrocarbons is comparable to the size of the zeolite cages. The presence of these hydrocarbon within the zeolite causes its lattice structure to expand during the reaction. Moreover, the intensity of the peaks is smaller for the spent catalyst. This shows that crystallinity of the catalyst decreases after the reaction. In Li et al.[14], it is explained that the crystallinity of the zeolite material deceases with increasing coke content as the spent catalyst contains not only H-SSZ-13 but also hydrocarbon material produced during the

reaction. The retention of hydrocarbons within the pores therefore affects both the framework and crystallinity of the catalyst.

3.1.2 Ammonia Temperature-Programmed Desorption

Ammonia Temperature-Programmed Desorption (NH_3-TPD) is an analytical technique used to determine the amount and the strength of the acid sites present within a zeolite catalyst. After being adsorbed within the pristine sample of H-SSZ-13, ammonia is desorbed during a constant temperature increase (from 100°C to 600°C)[10]. The TCD signal obtained as a function of temperature is plotted in Figure 5. Two desorption peaks are visible on this figure. A narrower peak around 200°C and a wider peak at 500°C. The peak at lower temperatures corresponds to ammonia that was either physically adsorbed or held by weak acids. The peak at higher temperatures corresponds to ammonia desorbed from stronger acid sites. According to Zhu et al.[15] and Borodina et al.[10], this is the expected NH_3-TPD results for the H-SSZ-13 zeolite. Furthermore, the acid site density found for the tested sample is 0.95 mmol/g which is slightly higher than expected by Borodina et al.[10].

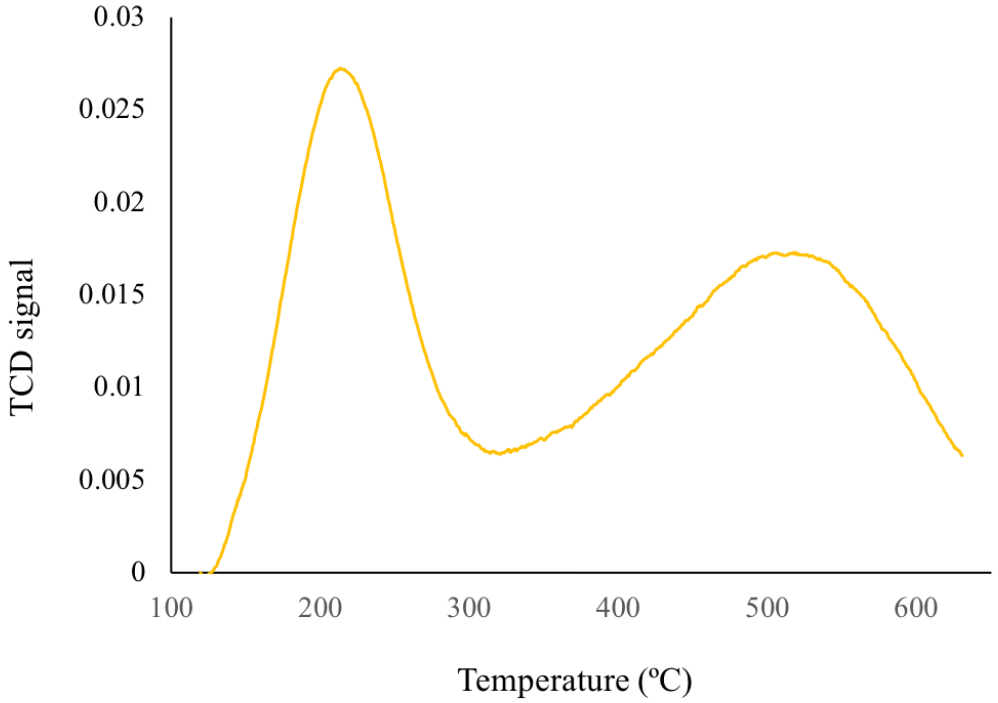

Figure 5: TCD signal for NH_3-TPD as a function of temperature for the fresh catalyst.

3.2 Variation of Reaction Parameters

Two types of gaseous products are observed after the experiments, olefins and parrafins, with olefins being the desired products. The alkene products consist of C_2 to C_5 olefins, while the alkane products consist of C_1 to C_4 parrafins. However, with different reaction conditions, the distribution of said products varies. The data extracted from the GC is presented in the following sections.

3.2.1 Influence of Reaction Temperature

The reaction temperature was varied according to the experiments presented in Table 1. The experiment at 470°C was repeated three times to check for reproducibility. It is important to know how reproducible an experiment is, so its experimental accuracy can be determined. To show this, the methanol conversion from all three experiments conducted at 470°C is plotted in Figure 6.

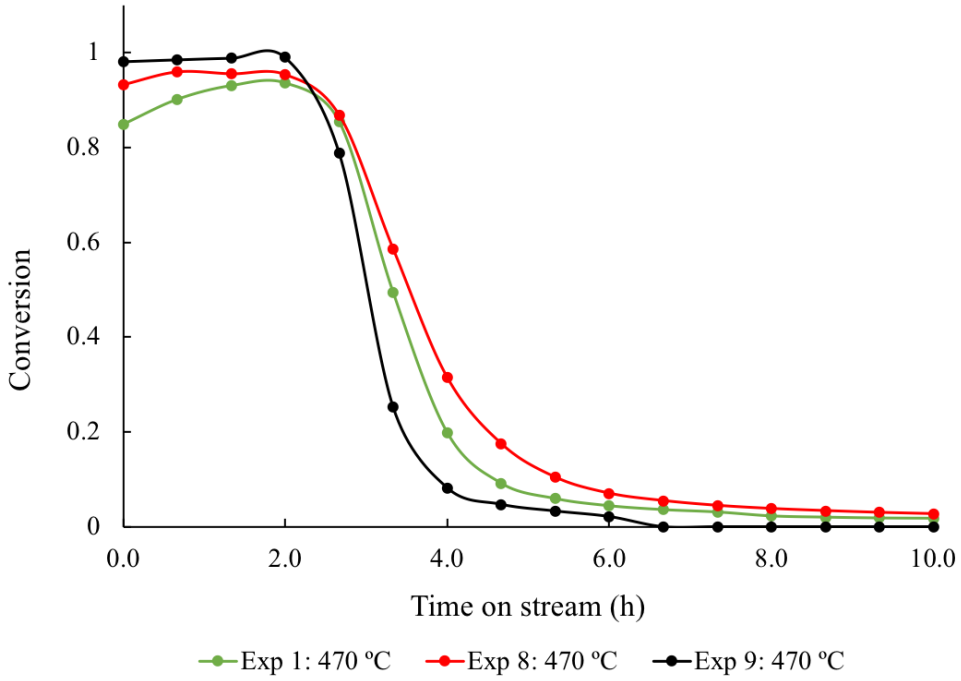

Figure 6: Methanol conversion for each experiment at 470°C.

For all three data sets, the conversion is highest at the start of the reaction, but then drops quite suddenly after about 2 hours on stream. This is called a "delayed breakthrough" trend [2]. The conversion curves for each experiment are not completely overlapped, meaning that there is some deviation between the results. The major difference in data points are at the beginning of the reaction and after 3.5 hours on stream, during the conversion decline. The percentage of deviation between the methanol conversion for each experiment can be seen in Figure 7. At 3.5 hours on stream, the deviation between Experiments 8 and 9 is highest, reaching 33%, while the deviation between experiments 1 and 9 reaches 25%. After 4 hours on stream, the deviation between Experiments 1 and 8 reaches 11%.

Experiment 1 and 8 are therefore closest in terms of reproducibility, however all experiments have quite a high degree of difference between them, leading to the conclusion that the experiment is not reproducible. To check whether this lack of reproducibility is due to human error during the experimental procedure or possibly due to the effect of higher temperature on the stability of the products, the experiment at a lower temperature (390°C) could have been repeated.

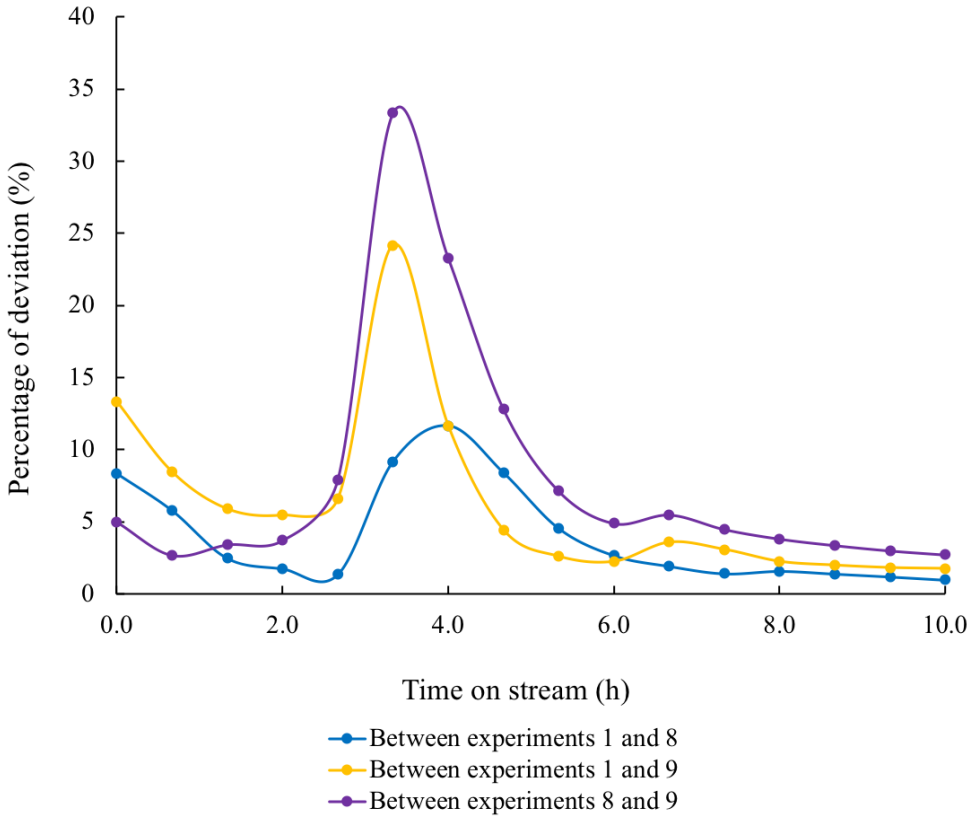

Figure 7: Methanol conversion deviation (in %) between all experiments performed at 470°C.

The methanol conversions, as a function of time on stream, for all tested temperatures from Table 1 are also compared in Figure 8. Note that the data from the first experiment at 470°C is used in this plot and for all following discussion. The conversion at 470°C is slightly lower and decreases faster than the conversions at 390°C and 430°C. For the three highest temperatures, similar to what is shown in Figure 5, the conversion at the start of the reaction is the highest and above 80%. The conversion at 430°C reaches the maximal conversion of 100%. The conversion at 350°C however, is only maximal for an 1 hour before dropping drastically to less than 10%. Multiple previous publications report similar results at lower temperatures [10][16][17]. This short catalytic life time at 350°C can be explained by taking a look at the dual-cycle mechanism seen in Figure 2. It has been proven by Z.Shi et al.[18] that at lower temperatures, the olefin-based cycle is dominant and at higher temperature the arene-based

cycle is dominant. At lower temperatures, such as 350°C, the dealkylation of the polymethylbenzenes in the aromatic-based cycle is not possible [19]. These species then accumulate, meaning there are less aromatic species in the hydrocarbon pool to be methylated, causing the catalytic pores to be blocked and consequently causing deactivation. On the contrary, at 470°C, the catalytic lifetime is lower due to the faster rate of coking [17]. As at higher temperature the aromatic-based cycle is preferred, the polyaromatic coke precursors are formed quicker [10].

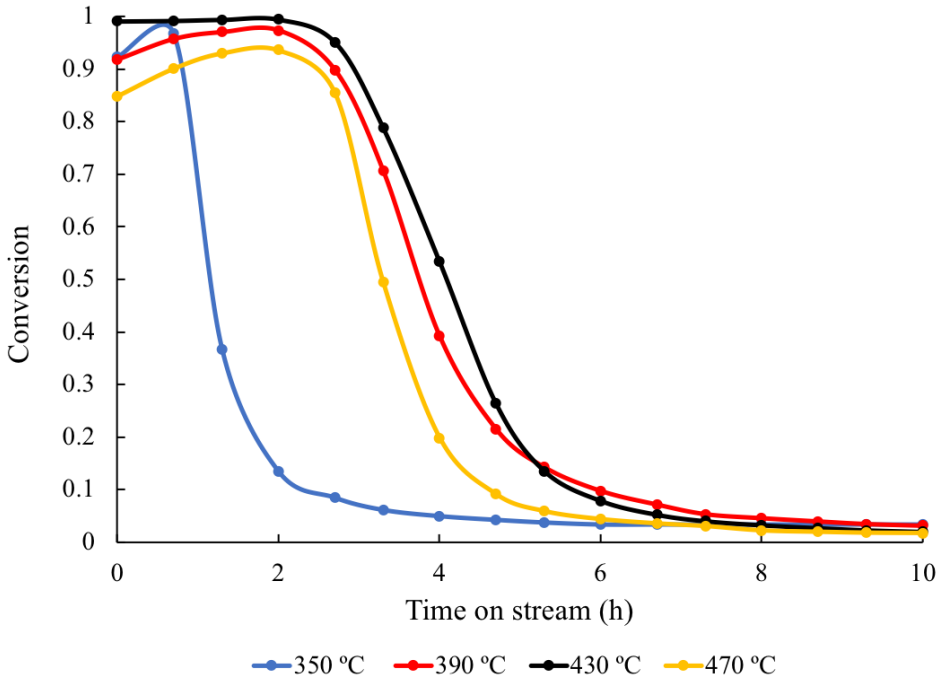

Figure 8: Methanol conversion as a function of time on stream for all tested reaction temperatures.

Alongside the methanol conversion, the products obtained during the MTO reaction are analysed as well. The composition of the product stream after 1.3 and 8 hours, for each temperature, is shown in Figure 9. A few interesting aspects about the product distribution can be observed in this figure. First, at shorter times on stream there are more products, including parrafins, than at higher times on stream, which is in accordance with the decreasing conversion. The main alkene products are indeed C_2 to C_4 olefins, with some C_5 olefin at higher temperatures. The main alkane side product is propane, which is in agreement with U.Olsbye et al.[2]. The alkane products are only present at the start of the reaction. This is because they are formed through hydrogen transfer, which is favored at shorter times on stream [20]. After 8 hours, the only products in the product stream are ethylene and propylene (and methane at 470°C). This shows that even after a longer times on stream, the catalyst is not completely deactivated. Even though the catalytic channels may be completely blocked, H-SSZ-13 retains some activity due to the presence of active sites on its surface [21].

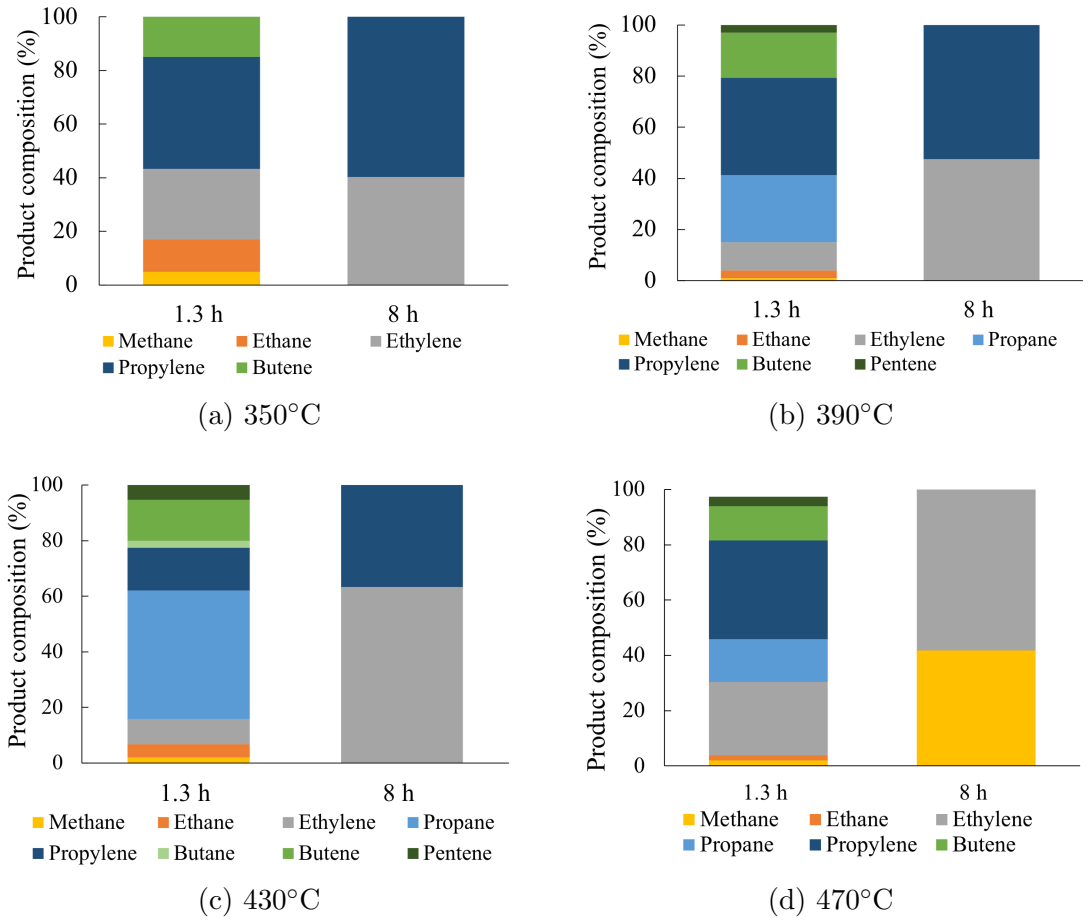

(a) 350°C (b) 390°C

(c) 430°C (d) 470°C

Figure 9: Product composition of the gas stream for each tested reaction temperature.

Lastly, as ethylene and propylene are the main olefin products, their selectivity is discussed in more detail below. In Figure 10, the ethylene to propylene ratio for each tested temperature is plotted. As a general trend, the ethylene to propylene ratio increases with increasing reaction temperature and increasing time on stream. At the lowest temperature, 350°C, the ratio stagnates around 0.6, after a sudden peak after 1 hour on stream. At the highest temperature, 470°C, the ratio keeps rising up to 2.8 at 7 hours on stream. The ratio drops to zero after this as there is no more propylene being produced. The ratios in Figure 10 reveal that at lower temperatures propylene is favored and at higher temperatures, ethylene is favored. This is again due to the favored mechanistic cycle at lower versus higher temperatures, as propylene is the main product of the olefin-based cycle and ethylene is the main product of the aromatic-based cycle (see Figure 2) [2][7]. As at higher temperatures the aromatic-based mechanism is favored, the increase of selectivity towards ethylene is justified and is in line with Shi et al.[18]. Moreover, the largest difference between these ratios is at the longer times on stream, meaning that ethylene is favored after a longer time on stream, when the catalyst is reaching complete deactivation. The detailed selectivities

for each olefin product can be found in Appendix C.2.1.

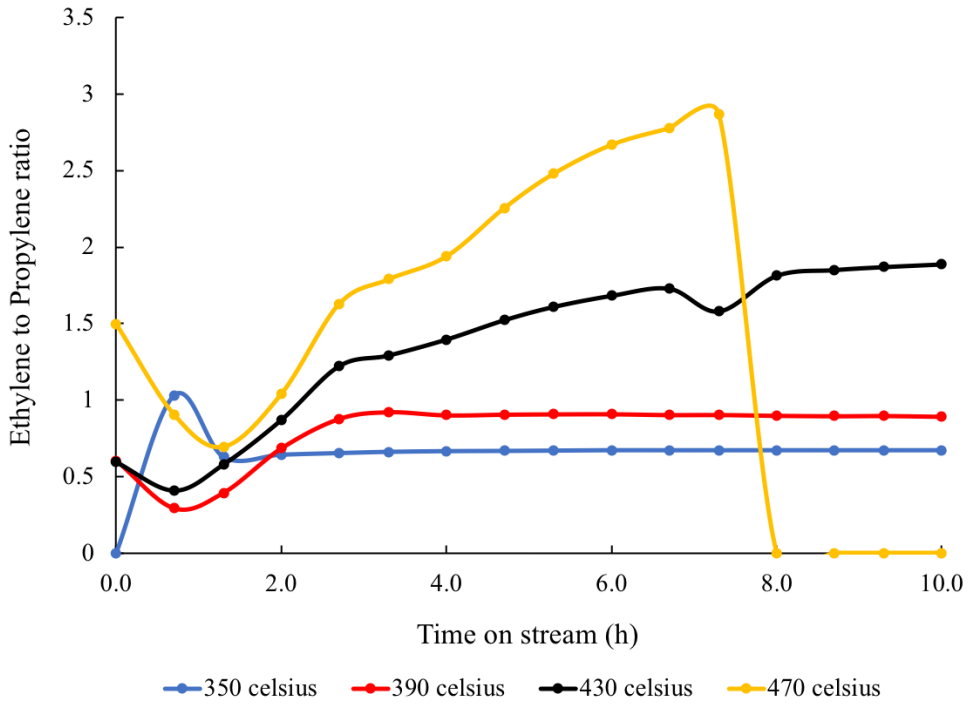

Figure 10: Ethylene to propylene ratio as a function of time on stream.

At 390°C, 430°C and 470°C the methanol conversion is very similar. However, the main difference between these reaction temperatures is in their olefin product distributions. Depending on which olefin is desired, the optimal reaction temperature can be selected.

3.2.2 Influence of Weight Hourly Space Velocity (WHSV)

The WHSV is defined by Equation (8) in *"2.2 Reaction condition testing"*. This equation shows that for the same methanol mass flow rate, the WHSV decreases with increasing catalyst loading. Three experiments regarding WHSV were preformed (see Table 1). Similar to the reaction temperature experiments, the methanol conversion indeed varied with WHSV. From Figure 11, it is seen that the methanol conversion increases with decreasing WHSV. For both 1.03 h^{-1} and 0.77 h^{-1}, the conversion reaches maximal conversion at the start of the reaction. At 1.03 h^{-1}, the conversion drops after 3 hours on stream while at 0.77 h^{-1} the conversion drops after 4 hours on stream. At the highest WHSV of 1.54 h^{-1}, the conversion only reaches 80% at its maximum and drops after 2 hours on stream. Therefore, it is seen that with decreasing WHSV, the catalytic lifetime increases. Catalyst lifetime is dependent on the contact time, which is defined as the mass of the catalyst divided by the methanol flow rate. When the WHSV decreases, the contact time increases. This is because as the catalyst loading increases, so does the amount of active sites present within the catalyst. There are then more active sites by where methanol can be converted to product. The conversion is therefore higher at higher contact times. This is explained by Kaarsholm et al. [22] and the trend confirmed by Wu et al.[16].

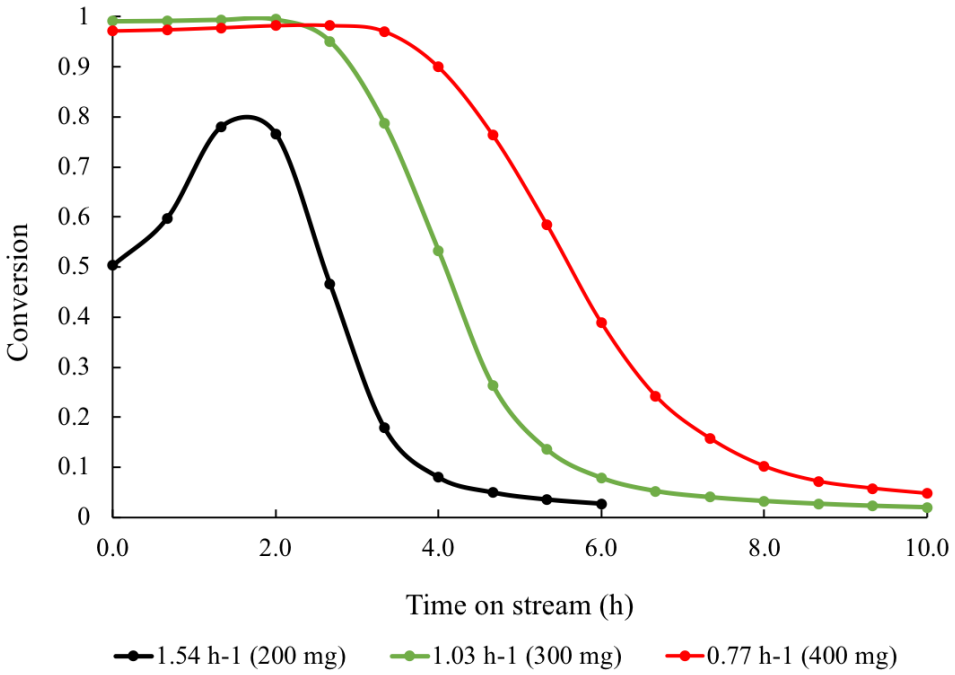

Figure 11: Methanol conversion for all tested WHSVs as a function of time on stream.

The product compositions for each tested WHSV are shown in Figure S2 in Appendix C.1.1 and follow the same trend as for the temperature experiments. The selectivity for each olefin at each WHSV can be seen in Figure S5 in Appendix

C.2.2. With decreasing WHSV, the selectivity towards ethylene decreases while the selectivity towards butene and pentene increases. In this next section however, the selectivity of alkenes versus alkanes is investigated. Figure 12 displays the lower olefin and paraffin selectivities for each tested WHSV.

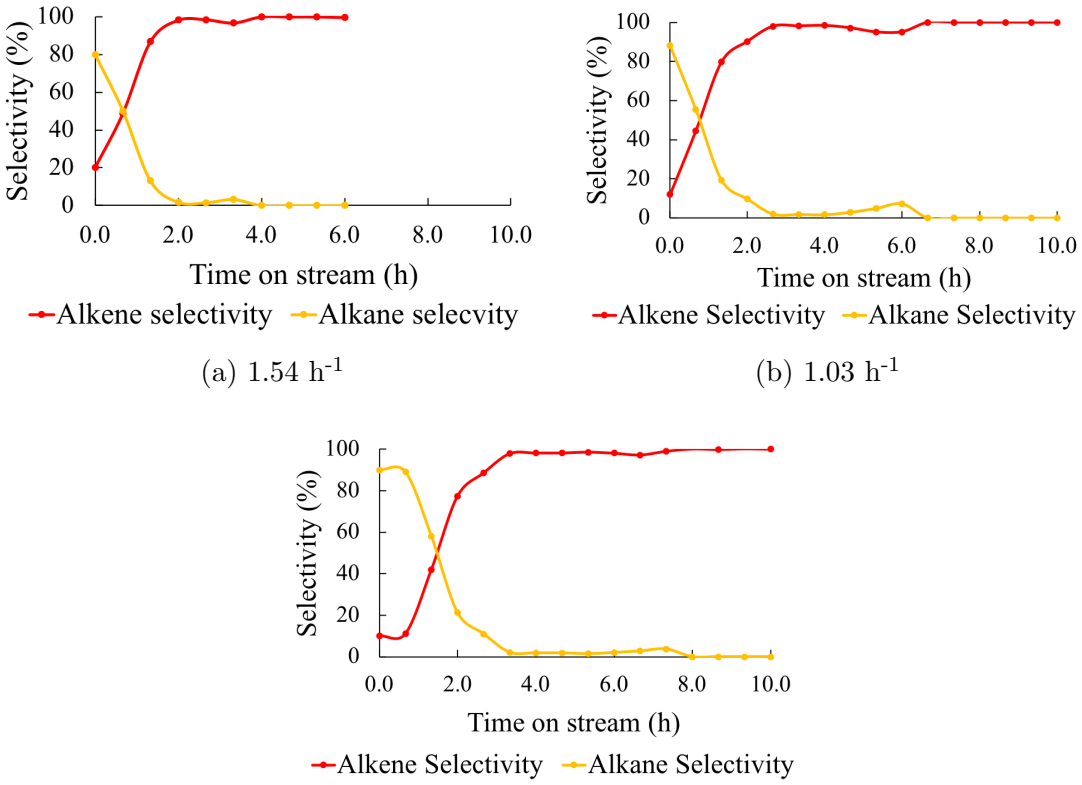

(a) 1.54 h^{-1}

(b) 1.03 h^{-1}

(c) 0.77 h^{-1}

Figure 12: Comparison of paraffin and olefin selectivities for each tested WHSV.

From the figure above it is observed that the selectivity towards parrafins decreases over time and the selectivity towards olefins increases. The formation of alkanes, which is due to intermolecular hydride transfer [20], is therefore favored towards the beginning of the reaction. At the lowest tested WHSV, 0.77 h^{-1}, the alkane selectivity stays at 90% for 1 hour on stream instead of instantly decreasing (which is the case for 1.54 h^{-1} and 1.03 h^{-1}). This is because at lower WHSV, there is a higher conversion of methanol, and therefore a higher portion of parrafins are obtained. This is in line with Wu et al.[16] and Shi et al.[18], where it is stated that with the higher methanol conversion at lower WHSVs also comes lower selectivity for olefins. Within the C_1 to C_4 alkanes, the selectivity towards propane is the largest, with an initial selectivity between 66% and 75% depending on the WHSV. This correlates with the fact that propylene is produced in the highest amount amongst the olefins.

3.2.3 Influence of Methanol Partial Pressure

The see the effects of methanol partial pressure on the catalytic performance and product stream composition, two partial pressures were compared (0.165 bar and 0.266 bar). As the partial pressure of methanol increases, the methanol flow rate does too. At the same catalyst loading and higher partial pressure, the WHSV would also change. Therefore to make sure that only the partial pressure is varied, the catalyst loading was adjusted (see Table 1). This ensured that for both partial pressure experiments, the WHSV was at 1.03 h^{-1}. As with the temperature and WHSV, the methanol conversion is plotted as a function of time on stream and shown in Figure 13.

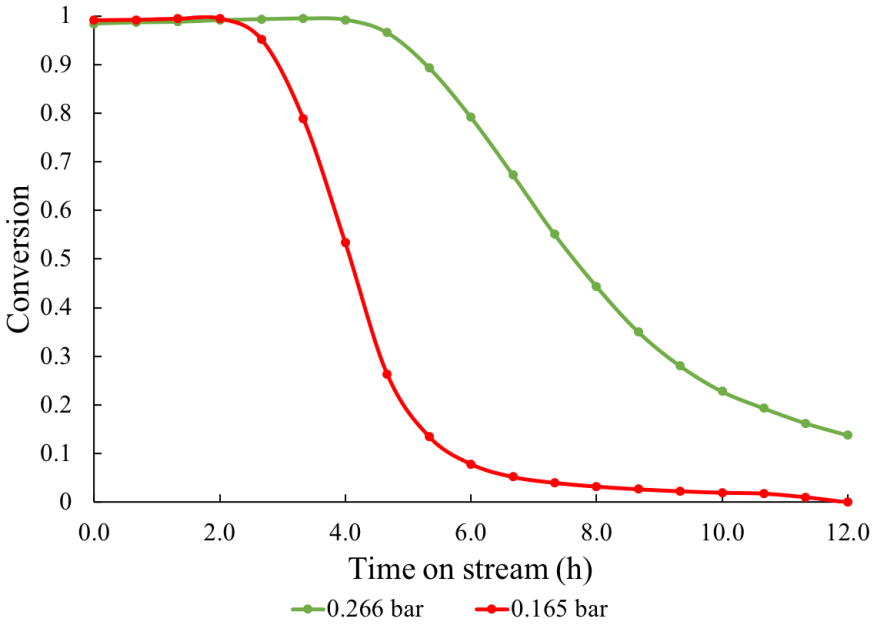

Figure 13: Methanol conversion for each methanol partial pressure as a function of time on stream.

From Figure 13, it is seen that at higher methanol partial pressure, the conversion of methanol is higher and stays higher for longer. At a partial pressure of 0.165 bar, the conversion is maximal until about 2.5 hours on stream, while at 0.266 bar, the conversion is maximal for 5 hours on stream. The maximal conversion time doubles as the methanol partial pressure increases by 0.1 bar. This increase in conversion is understandable as a higher partial pressure signifies a higher methanol flow rate. A higher concentration of methanol is going through the reactor, therefore more of it can be converted, which is consistent with Wu et al.[23]. Another aspect to be mentioned is the rate at which the conversion decreases. At 0.165 bar, the conversion of methanol drops quite drastically to below 10% after those 2.5 hours, yet at 0.266 bar, the conversion drops at a slower rate. Even after 12 hours on stream, the conversion at 0.266 bar only barely drops below to 20%. This can be explained by the higher catalyst load-

ing at 0.266 bar, and so the higher amount of catalytic sites and longer contact time. Overall, the general conversion trend of partial pressure in analogous to the trends for reaction temperature (higher conversion at higher temperatures) and WHSV (higher conversion for lower WHSV).

The product stream composition follows the same trend as for the reaction temperature and the plots can be seen in Figure S3 in Appendix C.1.2. Within the olefins products, the selectivity towards the C_2 - C_5 alkenes varies between the two tested methanol partial pressures. At 0.165 bar, the selectivity towards ethylene is higher and the selectivity towards butene and pentene are lower. However, at 0.266 bar, the ethylene selectivity is lower and that of butene and pentene are higher. The complete olefins selectivties are shown in Figure S6 Appendix C.2.3 and are similar to that of decreasing WHSV.

As mentioned, the butene selectivity increases with increasing methanol partial pressure. So far, butene has been discussed as one olefin. In reality, there are three butene isomers that are present in the product stream. The two constitutional isomers that are present are 1-Butene and 2-Butene. For the 2-Butene isomer, there is possibility of either a cis or trans orientation. The three butene molecules that occur in the product stream are presented below in Figure 14.

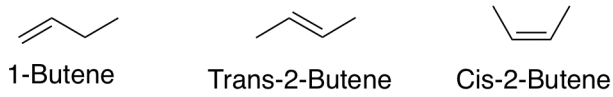

Figure 14: Butene isomers present in product stream.

The selectivity for each isomer is shown as a function of time on stream in Figure 15 and is calculated with Equation (12) from *"2.3 Product Analysis"*.

For both methanol partial pressures, the C_4 isomer selectivities follow a similar trend and have similar values. The selectivity towards 1-Butene decreases with time on stream while the selectivity towards 2-Butene increases. 1-Butene is less stable than 2-Butene [24], which explains why it becomes less favored as the reaction proceeds. As for the trans and cis isomers, the Trans-2-butene selectivity is higher than the Cis-2-butene selectivity. After rising at the beginning of the reaction, these selectivities seem to stagnate at around 40% and 25% respectively. For the trans isomer, there is less steric hindrance then for the cis isomer. The cis isomer therefore experiences more bond angle distortion [24]. Due to this, the cis molecule is less stable than the trans molecule. As the trans molecule is more stable, it becomes the more favored isomer, leading to its higher selectivity. This selectivity trend within the C_4 olefin is the same for all reaction temperatures and WHSVs.

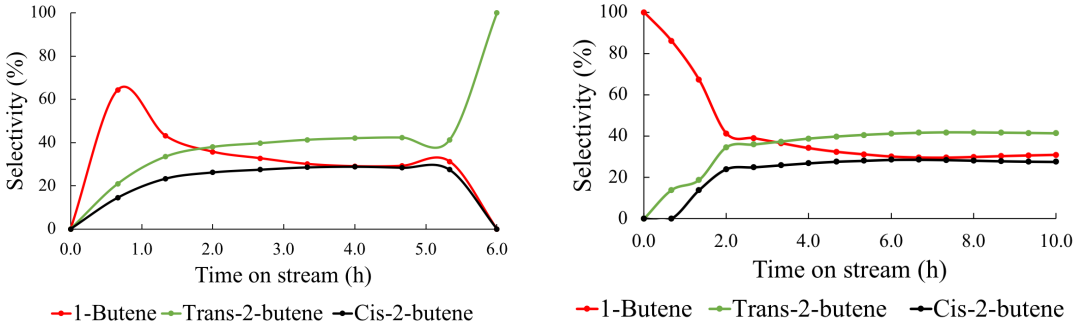

(a) 0.165 bar (b) 0.266 bar

Figure 15: Butene isomer selectivity as a function of time on stream for each methanol partial pressure.

3.3 Thermogravimetric Analysis

Thermogravimetric analysis (TGA) was preformed for Experiments 1 through 7 to compare the amount of coke formed in each case. TGA shows the weight loss of the spent catalyst as a function of increasing temperature. The higher the weight loss %, the more hydrocarbon material is retained within the catalyst. The catalyst weight loss for all experiments is plotted in Figure 16. For TGA analysis, there are three parts of the plot that are important. First, the weight drop from room temperature to about 100°C. This section corresponds to the weight loss due to the evaporation of water from the sample. Next, the weight loss from 100°C to 500°C corresponds to the decomposition of what is called "soft coke". This soft coke refers to the large aromatics confined within the catalyst [25]. This type of coke still has a high hydrogen content and does not lead to catalyst deactivation. Lastly, from 500°C to 600°C, the weight loss corresponds to the decomposition of hard coke, which is formed from soft coke via dehydrogenation. It therefore has a lower hydrogen content and is the reason for catalyst deactivation [26].

In Figure 16 (c), the weight loss of the spent catalyst is shown for the two tested methanol partial pressures (0.165 bar and 0.266 bar). For the sample tested at 0.266 bar, the slope of the weight loss between 100°C and 500°C is steeper than for the sample tested at 0.266 bar. This means that at a higher methanol partial pressure there is more soft coke formed than at lower partial pressure. From 500°C to 600°C, the slopes for both curves appear to be equal. The amount of hard coke is therefore assumed to be the same for both partial pressures. Even though there is a higher amount of soft coke at 0.266 bar, it does not lead to deactivation, which is in line with the longer catalytic lifetime at the higher tested partial pressure (see Figure 13 in *"3.2.2 Influence of Methanol Partial Pressure"*) This trend is also confirmed in Hu et al.[27].

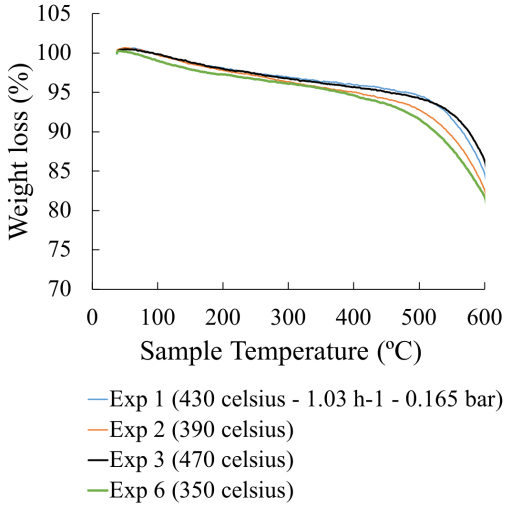

(a) Reaction temperature results

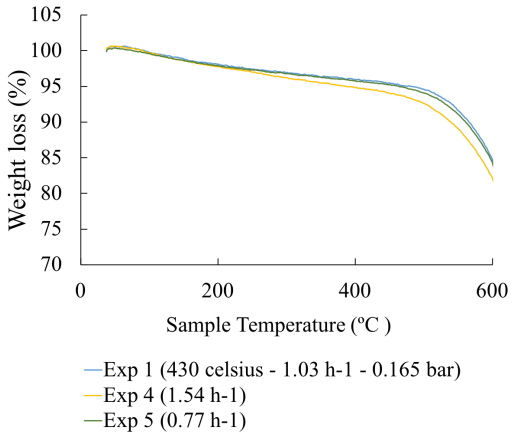

(b) WHSV results

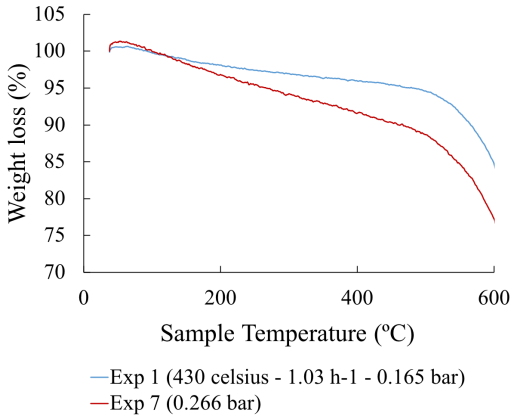

(c) Methanol partial pressure results

Figure 16: TGA results in terms on weight loss for all experiments.

In Figures 16 (a) and (b), the difference in weight loss is not as prominent. At a higher WHSV (1.54 h^{-1}) there is a slightly higher catalyst weight loss between 100°C and 500°C, indicating a higher amount of soft present. However, the slope indicative of the amount of hard coke is equal for all WHSVs. This poses an intrigue on the shorter catalytic lifetime at higher WHSV, as it is not explained by a difference in coke content. Hu et al.[28] explains that by increasing WHSV, the coking rate increases, meaning that even if the same amount of hard coke is formed for each experiment, the speed at which it is formed has an effect on catalytic deactivation.

As for the TGA results of the reaction temperature experiments, the weight loss between 100°C and 500°C is approximately the same for all reaction temperatures while between 500°C and 600°C, the weight loss increases with decreasing temperature. This indicates that the amount of soft coke formed for

each reaction temperature is similar, but the amount of hard coke increased with lower temperatures. It seems that even though the shorter catalytic lifetime at 470°C is due a faster rate of coking (see section *"3.2.1 Influence of Reaction Temperature"*) , it does not mean that a higher amount of coke is formed. In general, the influence of the reaction temperature on the phenomena of coking is quite complex [27]. Certain studies (Borodina et al.[10]) report that coking increase with increasing temperature, while others (Grønvold et al.[29]) report that coking increases with decreasing temperature. In this research the aspect becomes even more complicated as the repeated experiments at 470°C are not reproducible. However, what is visible is the difference in physical appearance of the spent catalyst after each experiment. At lower temperatures, the spent catalyst appears to have a lighter brown color while at higher temperatures it appears a darker brown, almost black color. This suggests that at different temperatures, the hydrocarbon species formed and trapped within the catalyst are different [27].

4 Conclusion

During this research, the influence of different reaction conditions on the MTO process and its catalyst were investigated. First, the H-SSZ-13 commercial catalyst used during the research was analysed with XRD and NH_3-TPD. Using XRD, it was confirmed that the catalyst has a framework and crystallinity associated with the CHA topology. NH_3-TPD allowed for the confirmation of the expected strong and weak acid sites within the zeolite.

Furthermore, by changing the reaction temperature, WHSV and methanol partial pressure, the methanol conversion, catalytic lifetime and product compositions were found to vary. Methanol conversion increases quite straightforwardly with decreasing WHSV and increasing methanol partial pressure. However, when varying the reaction temperature, the methanol conversion was best at intermediate temperatures (390°C and 430°C). At 350°C and 470°C, the conversion was maximal for a shorter period of time. The three experiments at 470°C were also not reproducible, leading to the results being different each time the experiment was repeated. Within the olefin products, for all reaction conditions, propylene was favored at the beginning of the reaction. Ethylene selectivity however increased with time on stream. Butene and pentene selectivities increased with lower WHSVs and higher methanol partial pressure and were highest for intermediate reaction temperatures. This correlates with the catalytic life time trends. Furthermore, the major side products of the reaction were indeed found to be alkanes. The paraffin products however become less favored as the reaction proceeded, with their selectivities dropping to below 10% after a few hours on stream. Lastly, for all experiments, the selectivity towards Trans-2-butene is the highest for all butene isomers and rises at the start of the reaction while the selectivity towards 1-Butene decreases throughout the reaction.

Lastly, the spent catalyst after reaction was analysed by XRD and TGA. The XRD analysis of the spent catalyst at 470°C identified that the framework of the catalyst is slightly shifted due to the formation of larger hydrocarbon molecules within the zeolite. Its crystallinity also decrease due the coke formation. The effect of the reaction conditions on the coking phenomenon on the first 7 experiments was analysed with TGA. The retained hydrocarbon material within the catalyst was distinguished between soft and hard coke. The trends between coke content allowed for the explanation and understanding of the catalytic life time trends for all tested conditions. Therefore, depending on the desired olefin product, the catalytic life time can be tuned by selecting the ideal reaction conditions.

5 Acknowledgments

The following people are acknowledged and thanked for their help during this research.
Jingxiu Xie as the main supervisor.
Peter J. Deuss as the second supervisor.
Henk van de Bovenkamp as the technician responsible for the set up.
Zahra Asgar Pour and Hamoon Hemmatpour as the analysis teaching assistants.
Bart de Jong, Martijn Hoving, Lisl Miedema and Loek Pieke as lab supervisors.

References

[1] P.Tian; Y.Wei; M.Ye; Z.Liu. "Methanol to Olefins (MTO): From Fundamentals to Commercialization". In: *ACS Catalysis* 5 (2015), pp. 1922–1938. DOI: 10.1021/acscatal.5b00007.

[2] F.Joensen; S.Bordiga U.Olsbye; S.velle; M.Bjørgen; P.Beato; T.V.W.Janssens and K.P.Lillerud. "Conversion of Methanol to Hydrocarbons: How ZeoliteCavity and Pore Size Controls Product Selectivity". In: *Angewandte Reviews* 51 (2012), pp. 5810–5831. DOI: 10.1002/anie.201103657.

[3] ACS Materials LLC. *SSZ-13 Zeolite*. 2018. URL: https://www.acsmaterial.com/blog-detail/ssz-13-zeolite.html (visited on 07/05/2022).

[4] Z.Xu; H.Ma; Y.Huang; W.Qian; H.Zhang and W.Ying. "Synthesis of Submicron SSZ-13 with Tunable Acidity by the Seed-Assisted Method and Its Performance and Coking Behavior in the MTO Reaction". In: *ACS Omega* 5 (2020), pp. 24 574 –24 583. DOI: 10.1021/acsomega.0c03075.

[5] J.Weitkamp. "Zeolites and catalysis". In: *Solid State Ionics* 131 (2000), pp. 175–188. DOI: 10.1016/S0167-2738(00)00632-9.

[6] Database of Zeolite Structures. *Framework type CHA*. 2017. URL: https://europe.iza-structure.org/IZA-SC/framework.php?STC=CHA (visited on 07/05/2022).

[7] J.S.Martinez-Espin; M.Mortén; T.V.W.Janssens; S.Svelle; P.Beato and U.Olsbye. "New insights into catalyst deactivation and product distribution of zeolites in the methanolto-hydrocarbons (MTH) reaction with methanol and dimethyl ether feeds". In: *Catalysis Science and Technology* 7 (2017), pp. 2700–2716. DOI: 10.1039/c7cy00129k.

[8] I.M.Dahl and S.Kolboe. "On the Reaction Mechanism for Hydrocarbon Formation from Methanol over SAPO-34". In: *Journal of Catalysis* 149 (1994), pp. 458–464. DOI: 10.1006/jcat.1994.1312.

[9] M.Bjørgen; S.Svelle; F.Joensen; J.Nerlov; S.Kolboe; F.Bonino; L.Palumbo; S.Bordiga and U.Olsbye. "Conversion of methanol to hydrocarbons over zeolite H-ZSM-5: On the origin of the olefinic species". In: *Journal of Catalysis* 249 (2007), pp. 195–207. DOI: 10.1016/j.jcat.2007.04.006.

[10] E. Borodina; F. Meirer; I. Lezcano-Gonzalez; M. Mokhtar; A. M. Asiri; S. A. Al-Thabaiti; S. N. Basahel; J. Ruiz-Martinez; and B. M. Weckhuysen. "Influence of the Reaction Temperature on the Nature of the Active and Deactivating Species during Methanol to Olefins Conversion over H-SSZ-13". In: *ACS Catalysis* 5 (2015), pp. 992–1003. DOI: 10.1021/cs501345g.

[11] W.Dai; X.Sun; B.Tang; G.Wu; L.Liu; N.Guan and M.Hunger. "Verifying the mechanism of the ethene-to-propene conversion on zeolite H-SSZ-13". In: *Journal of Catalysis* 314 (2014), pp. 10–20. DOI: 10.1016/j.jcat.2014.03.006.

[12] B.D.CULLITY. *Elements of X-Ray Diffraction*. Reading, Massachusetts: Addison-Wesley Publishing Company INC., 1978.

[13] J.Goetze; I.Yarulina; J.Gascon; F.Kapteijn and B.M.Weckhuysen. "Revealing Lattice Expansion of Small-Pore Zeolite Catalysts during the Methanol-to-Olefins Process Using Combined Operando X-ray Diffraction and UVvis Spectroscopy". In: *ACS Catalysis* 8 (2018), pp. 2060–2070. DOI: 10.1021/acscatal.7b04129.

[14] D.Li; Z.Liu; Y.Liu and Y.Zhang. "The Role of Coke as the Crystal Structure Protective Agent in the Synthesis of CHA Zeolites from Spent MFI". In: *Catalysis Letters* 150 (2020), pp. 1741–1748. DOI: 10.1007/s10562-019-03068-z.

[15] Q.Zhu; J.N.Kundo; T.Tatsumi; S.Inagaki; R.Ohnuma; Y.Kubota; Y.Shimodaira; H.Kobayashi and K.Domen. "A Comparative Study of Methanol to Olefin over CHA and MTF Zeolites". In: *Journal of Physical Chemistry* 111 (2007), pp. 5409–5415. DOI: 10.1021/jp063172c.

[16] X.Wu; M.G.Abraha and R.G.Anthony. "Methanol conversion on SAPO-34: reaction condition for fixed-bed reactor". In: *Applied Catalysis* 260 (2004), pp. 63–69. DOI: 10.1016/j.apcata.2003.10.011.

[17] M.S.Ahmad; C.K.Cheng; P.Bhuyar; A.E.Atabani; A.Pugazhendhi; N.T.L Chi; T.Witoon; J.W.Lim and J.C.Juan. "Effect of reaction conditions on the lifetime of SAPO-34 catalysts in methanol to olefins process – A review". In: *Fuel* 283 (2021). DOI: 10.1016/j.fuel.2020.118851.

[18] Z.Shi and A.Bhan. "Tuning the ethylene-to-propylene ratio in methanol-to-olefins catalysis on window-cage type zeolites". In: *Journal of Catalysis* 395 (2021), pp. 266–272. DOI: 10.1016/j.jcat.2021.01.015.

[19] H.Schulz; K.Lau; and M.Claeys. "Kinetic regimes of zeolite deactivation and reanimation". In: *Applied Catalysis* 132 (1995), pp. 29–40. DOI: 10.1016/0926-860X(95)00128-X.

[20] C.Wang; Y.Wang and Z.Xie. "Insights into the reaction mechanism of methanol-to-olefins conversion in HSAPO-34 from first principles: Are olefins themselves the dominating hydrocarbon pool species?" In: *Journal of catalysis* 301 (2013), pp. 8–19. DOI: 10.1016/j.jcat.2013.01.024.

[21] M.Fadoni and L.Lucarelli. "Temperature programmed desorption, reduction, oxidation and flow chemisorption for the characterisation of heterogeneous catalysts. Theoretical aspects, instrumentation and applications". In: *Studies in Surface Science and Catalysis* 120 (1999), pp. 177–225. DOI: 10.1016/S0167.2991(99)80553.9.

[22] M.Kaarsholm; F.Joensen; J.Nerlov; R.Cenni; J.Chaouki and G.S.Patience. "Phosphorous modified ZSM-5: Deactivation and product distribution for MTO". In: *Chemical Engineering Science* 62 (2007), pp. 5527–5532. DOI: 10.1016/j.ces.2006.12.076.

[23] W.Wu; W.Guo; W.Xiao and M.Luo. "Methanol conversion to olefins (MTO) over H-ZSM-5: Evidence of product distribution governed by methanol conversion". In: *Fuel Processing Technology* 108 (2013), pp. 19–24. DOI: 10.1016/j.fuproc.2012.05.013.

[24] MA.Fox and J.K.Whitesell. *Organic Chemistry*. Sudbury, Massachusetts: Jones Bartlett Publishers, 2004.

[25] M.Diaz; E.Epelde; J.Vallecillos; S.Izaddoust; A.T.Aguayo and J.Bilbao. "Coke deactivation and regeneration of HZSM-5 zeolite catalysts in the oligomerization of 1-butene". In: *Applied Catalysis B: Environmental* 291 (2021). DOI: doi.org/10.1016/j.apcatb.2021.120076.

[26] C.L.Minh; C.Li and T.C.Brown. "Kinetics of coke combustion during temperature-programmed oxidation of deactivated cracking catalysts". In: *Studies in Surface Science and Catalysis* 111 (1997), pp. 383–390. DOI: doi.org/10.1016/S0167-2991(97)80178-4.

[27] H.Hu; F.Cao; W.Ying; Q.Sun and D.Fang. "Study of coke behaviour of catalyst during methanol-to-olefins process based on a special TGA reactor". In: *Chemical Engineering Journal* 160 (2010), pp. 770–778. DOI: 10.1016/j.cej.2010.04.017.

[28] H.Hu; W.Ying and D.Fang. "Reaction and deactivation kinetics of methanol-to-olefins process based on a special TGA reactor". In: *Journal of Natural Gas Chemistry* 19 (2010), pp. 409–416. DOI: 10.1016/S1003-9953(09)60097-9.

[29] A.Grønvold; K.Moljord; T.Dypvik and A.Holmen. "Conversion of Methanol to Lower Alkenes on Molecular Sieve Type Catalysts". In: *Studies in Surface Science and Catalysis* 81 (1994), pp. 399–404. DOI: doi.org/10.1016/S0167-2991(08)63902-6.

Appendix A Hazard and operability study

No.	Guide Word	Parameter	Deviation	Causes	Consequences	Safeguards	Action Required
1	No	Flow	No flow	Nitrogen tank is empty	No nitrogen flow, so no methanol flow	Check pressure and flow indicators	Shut off system and change nitrogen tank
2	Less	Pressure	Low pressure	Leakage	Pressure is too low, not enough methanol lead to the reactor	Check pressure indicators	Shut off system and check lines for leakage
3	More	Pressure	High pressure	Blocked valve	Pressure build-up in system, can cause bursting of reactor	Check pressure indicators	Shut off system and check all valves
4	Less	Temperature	Low temperature	Heater malfunction	Desired reaction conditions aren't reached (methanol may not reach boiling point)	Check temperature of inlet stream and reactor oven	Turn on/ replace all necessary heaters
5	More	Temperature	High temperature	Heater malfunction	Risk of damaging equipment and melting glass reactor	Check temperature of inlet stream and reactor oven	Turn off/ replace all necessary heaters
6	Reverse	Flow	Backflow	Blockage in system	Methanol, olefins and catalyst can end up in nitrogen lines	Check valves are installed to allow only one way flow	Make sure check valves are installed and working

Table 2: HAZOP Table

Appendix B X-Ray Diffraction pattern

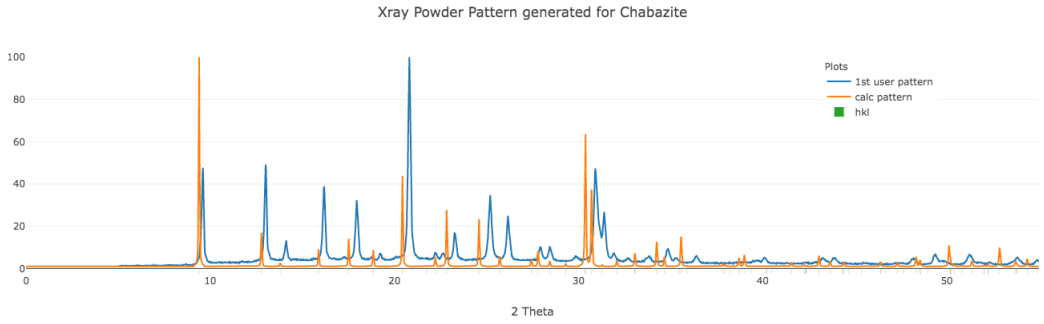

Figure S1: XRD patterns of a standard CHA zeolite and the SSZ-13 sample

The orange pattern represents the reference CHA framework while the blue pattern represents the tested H-SSZ-13 sample.

Appendix C Figures and Results

C.1 Product Distributions

C.1.1 Product Composition for WHSV experiments

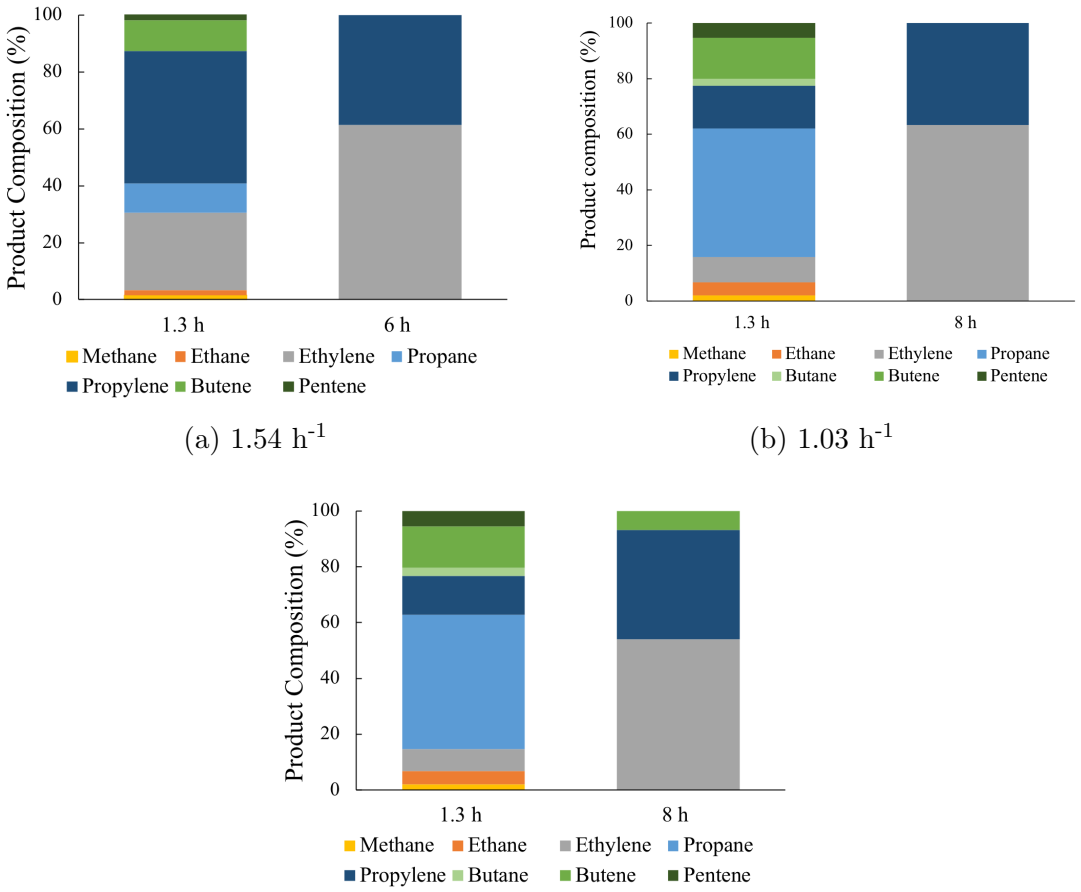

(a) 1.54 h^{-1}

(b) 1.03 h^{-1}

(c) 0.77 h^{-1}

Figure S2: Product compositions for each tested WHSV.

C.1.2 Product Composition of methanol partial pressure experiments

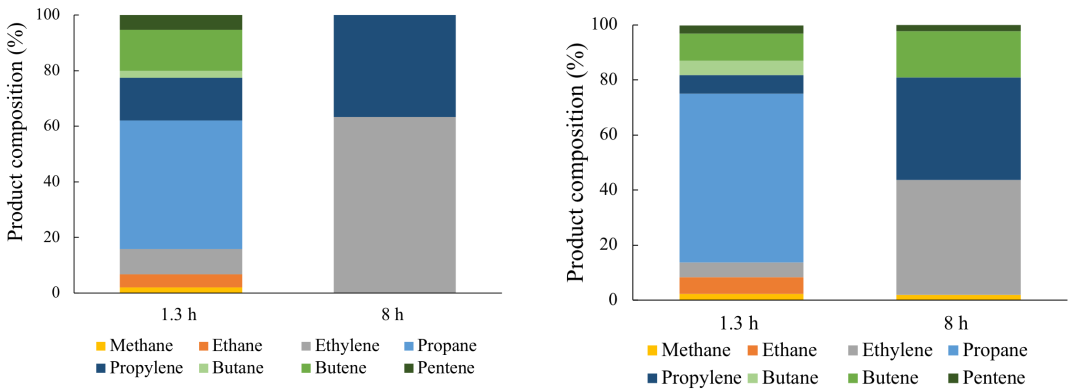

(a) 0.165 bar

(b) 0.266 bar

Figure S3: Product compositions for each tested methanol partial pressure.

Note that the graphs at 430°C, 1.03 h^{-1} and 0.165 bar are the same graph as they correspond to the results of Experiment 1 (from Table 1).

C.2 Olefin selectivities

C.2.1 Olefin selectivities for reaction temperatures

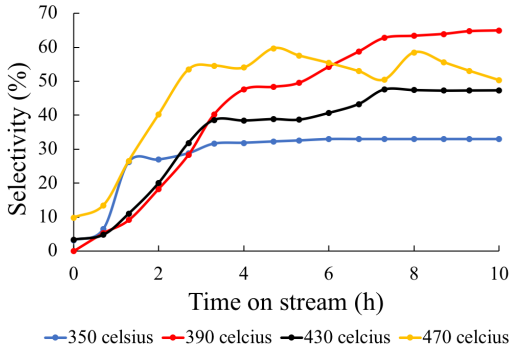

(a) Ethylene Selectivity

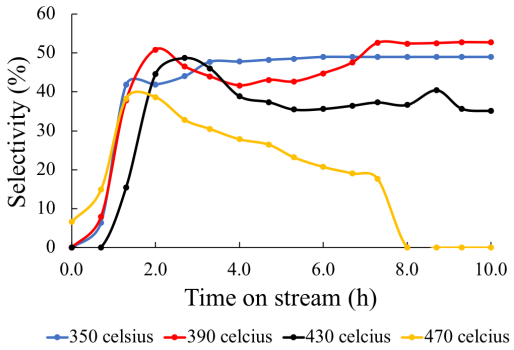

(b) Propylene Selectivity

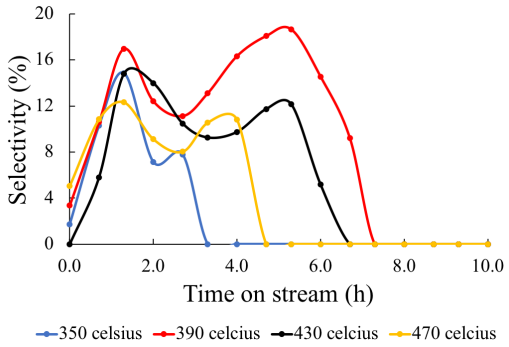

(c) Butene Selectivity

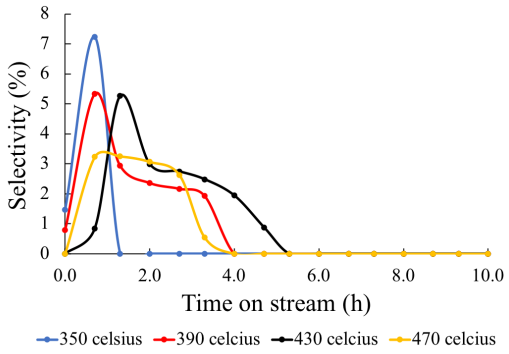

(d) Pentene Selectivity

Figure S4: Lower olefin selectivities as a function of time on stream for each reaction temperature.

C.2.2 Olefin selectivities for WHSVs

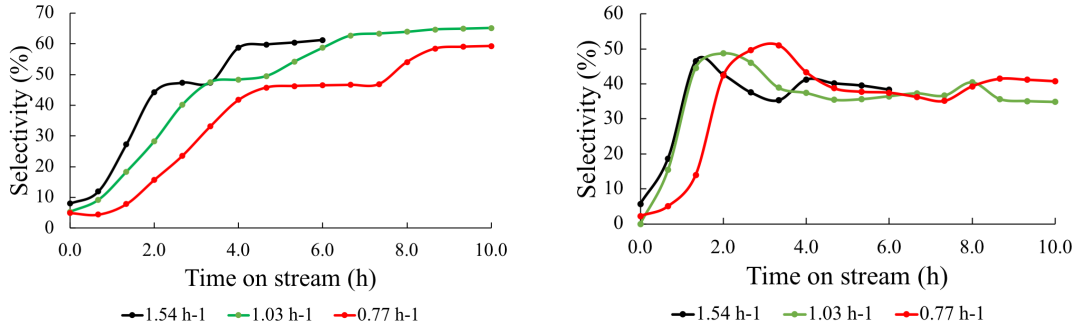

(a) Ethylene Selectivity

(b) Propylene Selectivity

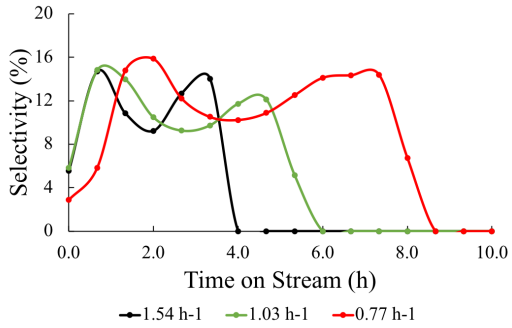

(c) Butene Selectivity

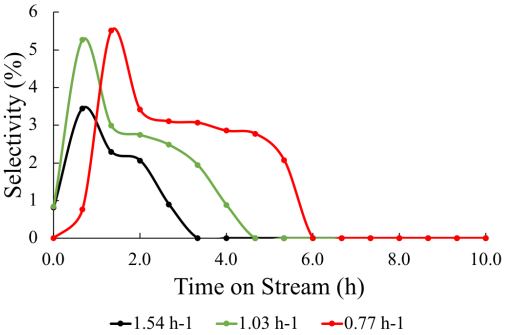

(d) Pentene Selectivity

Figure S5: Lower olefin selectivities as a function of time on stream for each WHSV.

C.2.3 Olefin selectivities for methanol partial pressure

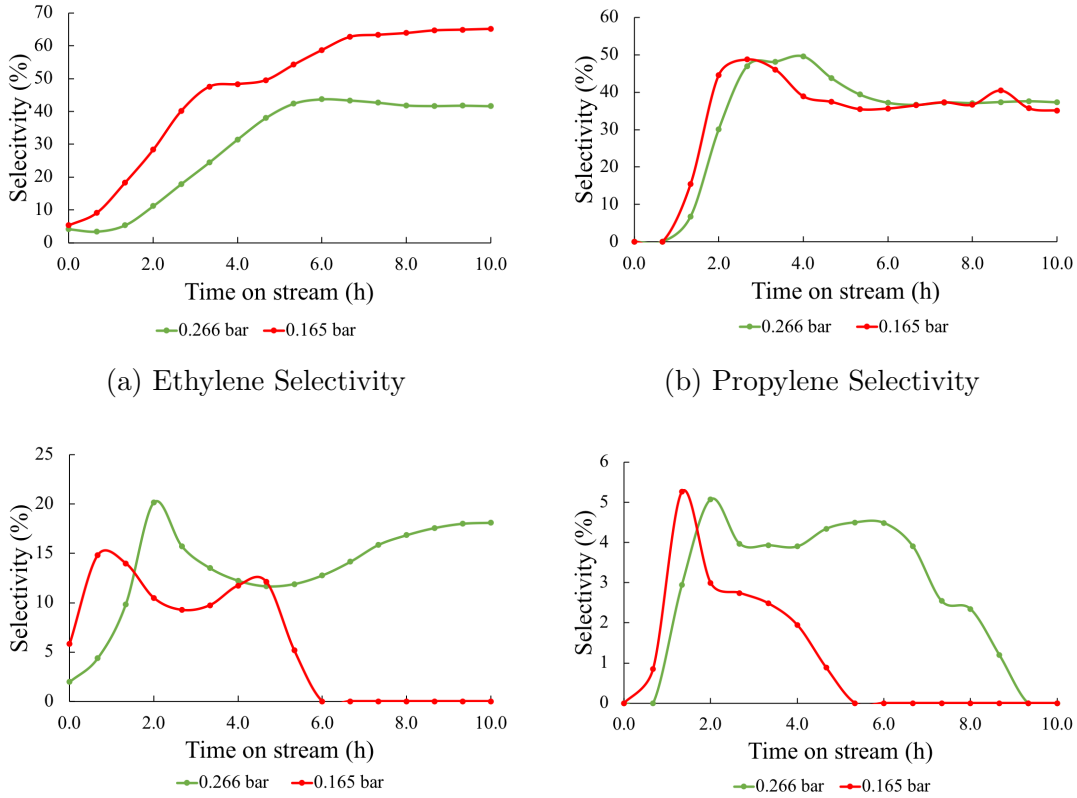

(a) Ethylene Selectivity

(b) Propylene Selectivity

(c) Butene Selectivity

(d) Pentene Selectivity

Figure S6: Lower olefin selectivities as a function of time on stream for each methanol partial pressure.

C.3 Alkane selectivities

C.3.1 Parrafin and olefin selectivities for all temperature experiments

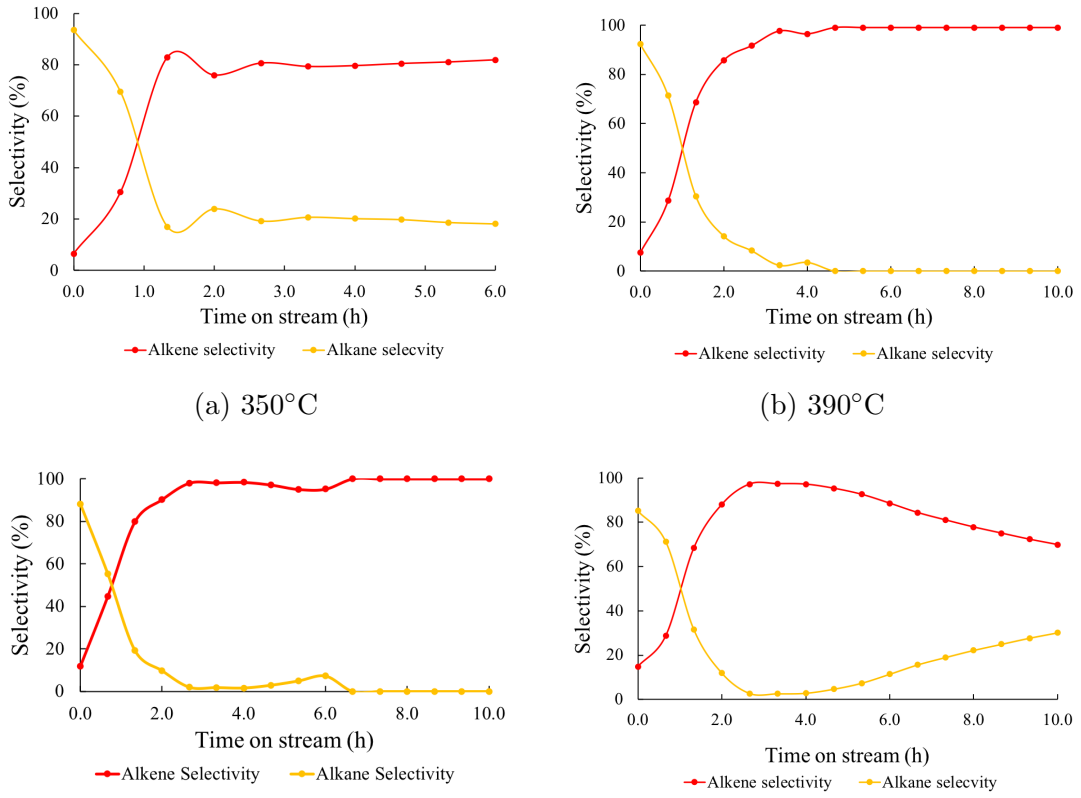

(a) 350°C

(b) 390°C

(c) 430°C

(d) 470°C

Figure S7: Comparison of paraffin and olefin selectivities as a function of time on stream for each reaction temperature.

C.3.2 Parrafin and olefin selectivities for all methanol partial pressure experiments

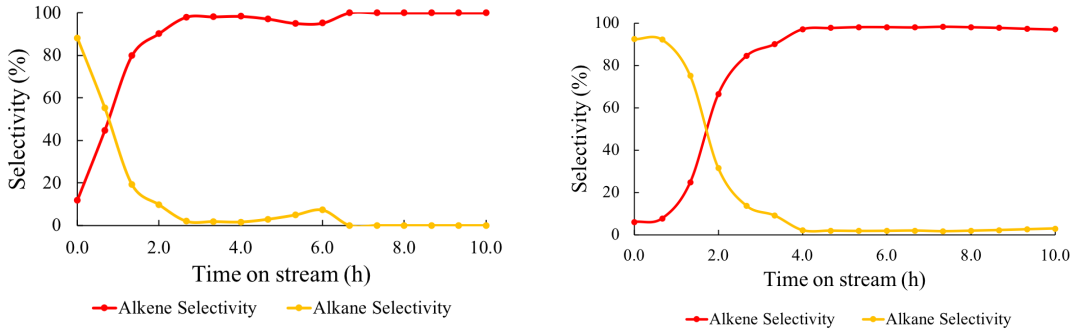

(a) 0.165 bar

(b) 0.266 bar

Figure S8: Comparison of paraffin and olefin selectivities as a function of time on stream for each methanol partial pressure.